

Hydrokinematic regions within the swash zone

Michael G. Hughes^{a,*}, Adrienne S. Moseley^b

^aUniversity of Sydney Institute of Marine Science, School of Geosciences, University of Sydney, NSW 2006, Australia

^bGeoscience Australia, GPO Box 378, Canberra ACT 2601, Australia

Received 12 September 2006; received in revised form 6 February 2007; accepted 22 April 2007

Available online 5 May 2007

Abstract

A method for delimiting the swash zone and regions within is presented. Two regions are recognized and distinguished by their differing flow kinematics. The outer swash region involves wave-swash interactions and related processes, whereas the inner swash region consists of pure swash motion (i.e., free from interaction with subsequent waves). The boundary between these two hydrokinematic regions can be determined from shoreline elevation time series. The vertical extent of the outer swash was found to scale directly with inner surf zone wave variance and beach slope. Since the vertical extent of the entire swash zone also varies directly with the former, the relative extents of the outer and inner swash are approximately constant for the range of beach slopes investigated here. The efficacy of a previously utilized method for determining the location of instruments in the swash zone, based on the percentage of time the bed is inundated, is established here for the first time. A new method for determining the location of an instrument station within either of the hydrokinematic regions is also presented, and requires only a single pressure sensor time series. The data discussed here include over 140 runup time series collected from five different sandy beaches with beach face gradients ranging from 0.03 to 0.12. The results are expected to be generally applicable to swell-dominated sandy beaches, where swash is driven by a combination of short and long waves in the inner surf zone. The applicability of the results at either extreme of the reflective–dissipative continuum remains to be established.

© 2007 Published by Elsevier Ltd.

Keywords: Swash; Wave runup; Shoreline; Wave-swash interactions; Beach face

1. Introduction

The swash zone is located between the continuously wet inner surf zone and the continuously dry sub-aerial beach. It is the zone that is periodically swept by shoreline motion, and is thus alternately submerged and dry. The mean position of the shoreline is approximately located where the mean water surface in the surf zone due to wave setup

intersects the beach face (Guza and Thornton, 1981; Nielsen, 1989). The shoreline motion about this mean position occurs in relation to waves of varying frequency (wind waves, swell, and infragravity waves) as well as the tide (Guza and Thornton, 1982; Hughes and Turner, 1999; Elfrink and Baldock, 2002). The term swash is generally used to collectively describe both the shoreline motion and the flow within the relatively thin lens of water that moves up and down the beach in connection with the shoreline (e.g., Hughes and Turner, 1999; Butt and Russell, 2000; Elfrink and Baldock, 2002; Masselink and Puleo, 2006).

*Corresponding author. Tel.: +61 2 9351 5190;
fax: +61 2 9351 0184.

E-mail address: michaelh@mail.usyd.edu.au (M.G. Hughes).

Recent studies of flow kinematics and sediment transport have identified clear differences in the nature of the outer and inner swash zone. For example, Masselink et al. (2005) reported the net sediment flux to be directed offshore in the outer swash (their ‘transition zone between inner surf and swash’) and onshore in the inner swash. Aagaard and Hughes (2006) reported similar results, but found that the net sediment flux in the outer swash could also be directed onshore if the beach face morphology included an inter-tidal bar. Aagaard and Hughes (2006) presented data showing that the turbulence structure can also differ between the outer and inner swash. Masselink and Russell (2006) demonstrated that the magnitude of the velocity skewness at their field sites was larger in the outer compared to the inner swash, but negative in both cases. All the three studies either imply or explicitly state that the outer swash included wave-swash interactions and the inner swash included only pure swash motion (i.e., free from interaction with subsequent waves). While it is clear that there are two distinct regions distinguished by their flow kinematics, nothing is presently known about the relative extents of these two regions and whether they vary according to beach type. Before this can be investigated further the boundary between these two hydrokinematic regions must be defined precisely.

Due to the randomness of natural waves, it can be difficult to successfully install fixed instrument stations to measure swash processes for any significant length of time. The extent and position of the swash zone varies considerably with each successive short wave (wind wave and swell) as well as with lower-frequency infragravity waves and tides. The fact that one swash cycle often does not complete before the arrival of the next wave complicates the situation further. A fixed instrument station on the beach face may at one time be experiencing only fluid motion due to swash and at other times it may be experiencing waves overrunning a preceding swash lens. Earlier on or later in the tide cycle it may be in the inner surf zone or on the subaerial beach. Such complications can confound the direct comparison of data at different times within the one-field deployment as well as between different beaches.

Given the differing nature of the outer and inner swash and the fixed location of instrument stations relative to the moving boundary between the two, it is important to describe where data was obtained

(instrument station was located) within the swash zone, but few studies have done this in a quantitative way. Those that have, determined the percentage of time that the instrument station (bed) was inundated to indicate approximate position (Masselink et al., 2005; Aagaard and Hughes, 2006). The premise being that a large percentage of time inundated means the instruments are located toward the seaward boundary of the swash zone and a small percentage of time inundated means they are located toward the landward boundary. The efficacy of this approach has not been established to date. The way that inundation time varies across the swash zone is unknown, as is its consistency across beach types. While this approach is useful to some extent, one drawback is that it does not explicitly indicate whether the instrument station is situated in either the outer or inner swash.

This paper identifies a means for delimiting the outer and inner swash regions, and investigates their relative extents. It establishes the efficacy of the presently available approach for identifying the location of an instrument station within the swash zone (viz., percentage of time the instruments are inundated), and also provides a new method for identifying where an instrument station is located relative to the outer or inner swash. These issues are addressed using field experiments measuring both the shoreline motion and water depth at many positions across the swash zone on a wide range of sandy beach types.

2. Definitions and concepts

2.1. Definition of terms

Fig. 1 defines the terms used throughout this paper. A *swash cycle* is defined in terms of shoreline oscillations and involves a single landward then seaward movement of the shoreline (Fig. 1a). There is no requirement for the shoreline to return to the original elevation. Swash cycles are, therefore, delimited by consecutive shoreline minima with one intervening shoreline maxima. On this basis there are three swash cycles shown in Fig. 1a. *Swash events* at a specified elevation on the beach face are defined by periods of bed immersion (water depths greater than zero), and separated by periods of zero water depth. The beginning of a local swash event is marked by a rise from zero water depth and the conclusion by a return to zero water depth. If there are no overrunning waves passing the specified

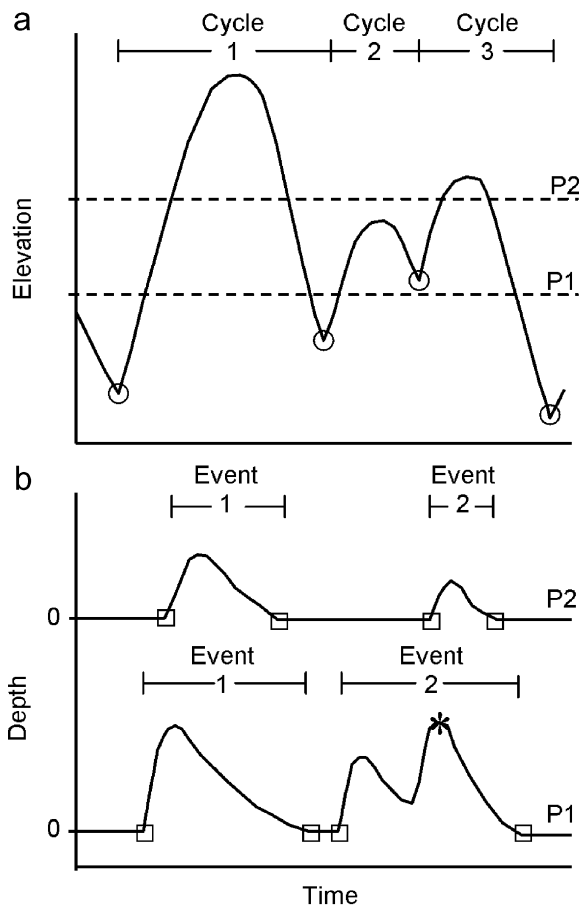


Fig. 1. Schematic diagram defining the terms used here to describe various swash parameters: (a) shoreline elevation time series and (b) water depth time series from two elevations P1 and P2 in (a). Scales are arbitrary. Note that P2 is landward of P1. Shoreline minima used to delimit *swash cycles* are indicated by circles. Local *swash events*, defined by periods of bed immersion, are delimited by squares. Overrunning waves defined by secondary peaks within a local swash event are indicated by asterisks.

position during the swash event, there will be one water depth maximum (wave) associated with the swash event, otherwise there will be two or more water depth maxima (waves). On this basis there are two local swash events shown in Fig. 1b at locations P1 and P2 (note that P2 is landward of P1). The second swash event recorded at P1 involves two waves, thus wave-swash interaction is occurring at that elevation. Note that the corresponding swash event at P2 involves only one wave, thus the overrunning wave recorded at P1 does not reach this elevation and there is only pure swash motion. The distinction between the terms *swash cycle* and *swash event* is an important one in this paper. Swash cycles relate to the shoreline motion and are

identified from a shoreline elevation time series. Swash events are location specific and are identified from a water depth time series measured at a specified elevation.

The *swash zone* is defined here as the zone, where the bed is alternately covered (wet) and uncovered (dry) by water in a specified time period that includes all sub-tidal frequencies of shoreline oscillation, but is stationary with respect to the tide. The *outer swash* is defined as the region, where wave-swash interactions are occurring and thus the number of water depth maxima (waves) is greater than the number of swash events over the specified time period. The *inner swash* is defined as the region, where wave-swash interactions are entirely absent and thus the number of water depth maxima (waves) equals the number of swash events in the specified time period.

2.2. Types of wave-swash interaction

There is no requirement for the number of swash cycles to match the number of local swash events (e.g., Hegge and Eliot, 1991; Weir et al., 2006). The number of swash events recorded depends on the elevation in the swash zone and the location and extent of wave-swash interactions. Three principal types of wave-swash interaction are illustrated in Fig. 2. (1) Wave capture, in which a wave traveling over an existing swash lens is overtaken by a following wave (Fig. 2a), (2) wave-uprush interaction, in which an incoming wave crosses the front of a swash lens while it is advancing up the beach (Fig. 2b), (3a) weak wave-backwash interaction, in which an incoming wave advances across the front of an existing swash lens as it is receding down the beach as backwash (these are not readily identifiable from still photographs), and (3b) strong wave-backwash interaction, which is similar to (3a), but it results in a stationary hydraulic jump near the seaward edge of the swash zone (Fig. 2c). While some of these types of wave-swash interaction produce a typical response in pressure sensor time series of water depth, unfortunately, there is no unique match between time series behavior and interaction type.

3. Field methods and data pre-processing

3.1. Field sites

This study draws from several data sets collected along the eastern seaboard of Australia, which is

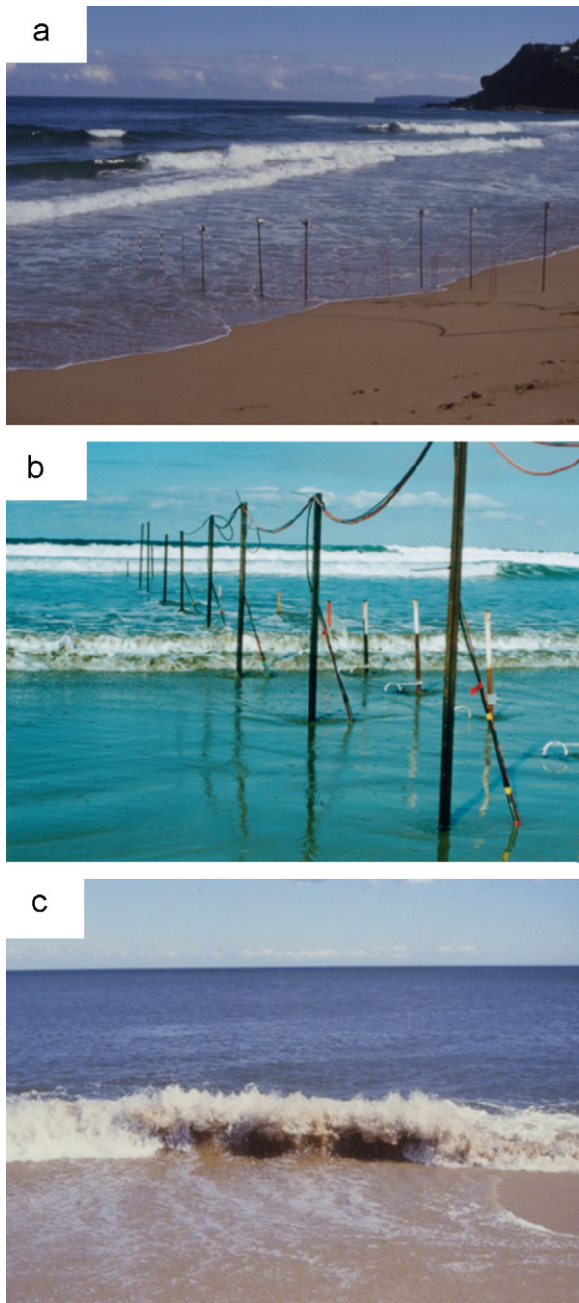


Fig. 2. Photographs showing examples of the various types of wave-swash interactions: (a) type 1, (b) type 2, and (c) type 3b. See text for descriptions of each type.

exposed to a moderate-energy, swell-dominated wave climate. The beaches studied display varying sediment sizes and degrees of exposure to the wave climate, thus a wide range of beach types (from reflective through to dissipative; see Wright and Short, 1984), beach face gradients, and wave breaker conditions are represented (Table 1). All

the beaches included are micro-tidal and semi-diurnal with a mean spring range of approximately 1.5 m.

3.2. Field setup

Each experiment was conducted over a semi-diurnal tide cycle commencing and finishing at low tide. A resistance-type runup wire was installed across the beach, extending from the inner surf zone to beyond the maximum runup location (e.g., Guza and Thornton, 1982). Adjacent to the runup wire a shore-normal array of between nine and 15 pressure sensors was installed. The runup wire provided time series of the shoreline location and the pressure sensors provided time series of the local water depth throughout the experiment. The runup wire was maintained at approximately 0.02–0.03 m above the bed, which required continual adjustment by an observer. This elevation is expected to provide results consistent with those from video techniques (Holland et al., 1995). A pressure sensor was also deployed just seaward of the swash zone in the inner surf zone. All instruments were logged at 10 Hz. The runup wire was calibrated by shorting the wire at surveyed positions along its length, and the pressure sensors were calibrated on site for hydrostatic water depth. The beach profile and locations of all instruments were surveyed either at the beginning or the end of the experiment, and frequently both.

3.3. Data pre-processing

For a spring tide range of 1.5 m (most experiments were performed over smaller tide ranges), the maximum tidal variation in water level over 15 min is approximately 6 cm, which is much smaller than the shoreline excursions measured. A period of 15 min is therefore considered to be stationary with respect to tidal variation in water level. For consistency across the entire data set, time series from all beaches were divided up into 15 min run lengths, which included at least seven (and sometimes up to 30) infragravity wave cycles if present, and of the order of 100 short wave cycles. The shoreline positions from the runup wire were converted to vertical elevation above the seaward end of the runup wire using the beach face gradient. The beach face gradient was measured as the planar slope on the surveyed beach profile between the highest shoreline maxima and lowest shoreline minima recorded for each 15 min data run. Power

Table 1

Summary of experimental conditions at each site: D_{50} is the median grain diameter, $\tan \beta$ is the beach gradient, H_b is the breaker height, T is the wave period, and ξ_b is the Iribarren number calculated using $\xi_b = \tan \beta / \sqrt{H_b/L_o}$, where $L_o = gT^2/2\pi$

Site	Date	D_{50} (mm)	$\tan \beta$	H_b (m) ^a	T (s) ^b	ξ_b ^c
Avoca Beach	14.10.03	0.55	0.121	0.58	12.7	1.05
Avoca Beach	16.11.04	0.85	0.072	0.80	10.7	1.13
Avoca Beach	17.11.04	0.85	0.082	0.76	11.6	1.40
Moreton Island	06.12.04	0.25	0.048	0.45	10.0	0.37
Pearl Beach (cusp horn)	26.03.98	0.33–0.62	0.108	0.49	12.0	1.33
Pearl Beach (cusp bay)	26.03.98	0.31–0.62	0.098	0.50	12.0	1.00
Seven Mile Beach	21.07.04	0.18	0.030	0.70	10.6	0.48
Seven Mile Beach	22.07.04	0.18	0.031	0.70	14.3	0.66
Stradbroke Island	06.11.01	0.28	0.038	0.51	11.5	0.35

^aMeasured in the inner surf zone.

^bDetermined from the spectral peak in the short wave band (measured in the inner surf zone).

^c $\xi_b < 0.64$ spilling breakers, $0.64 < \xi_b < 5.0$ plunging breakers, $\xi_b > 5.0$ surging breakers (Balsillie, 1985).

spectra calculated from inner surf zone water level and shoreline elevation time series had 22 degrees of freedom and a spectral resolution of 0.0011 Hz.

The analysis performed here required the identification and tallying of all shoreline maxima and minima in each runup wire time series and all wave crests in each pressure time series. Shoreline maxima and wave crests were automatically identified by zero-down crossings of the first derivative of the respective time series. Shoreline minima were then identified as the minimum shoreline elevation between successive shoreline maxima. Short durations between maxima in the records related to noise, such as small water surface ripples unrelated to the prominent short wave frequency band, were removed from the analysis by applying a threshold criterion of 2.5 or 5 cm in the vertical. The exact value used depended on the wave conditions and beach slope. The lower (higher) threshold was applied to beaches with a gradient less (greater) than 0.05 with small (large) wave heights arriving at the shoreline. Individual waves and shoreline excursions were only included in the data analysis if their height and vertical extent exceeded the chosen threshold.

4. Results

4.1. Delimiting the swash zone

An example swash time series is shown in Fig. 3. In this example, the relative shoreline excursion reaches up to 0.9 m in vertical elevation and water depth records are available from nine locations

within this excursion distance. The water depth records from locations below approximately 0.65 m elevation show several waves arriving during each swash event. That is, contained between the time period of one shoreline excursion up and then down the beach, several peaks occur in the water depth records indicating the passage of waves moving over the pre-existing swash lens. The same thing is evident in pixel intensity time stacks from video imagery of the swash zone where the paths of overrunning bores are seen on the surface of the swash lens, but do not reach the shoreline (see Aagaard and Holm, 1989; Holland et al., 1995). At elevations greater than 0.65 m (i.e., the highest two traces) there is only one peak in the water depth records for each shoreline oscillation. The water depth variation in these cases is simply due to the passage of the swash lens, absent from any interaction with subsequent waves. It is evident from this figure that elevations on the beach between 0.1 and 0.65 m at any instant may be subjected to swash, surf, or an interaction of the two.

From a theoretical flow kinematics viewpoint, the swash process begins when the shoreline begins to move landward from an initially still position, at least in the case of an incident bore or solitary wave (see Shen and Meyer, 1963; Yeh and Ghazali, 1988; Synolakis, 1987). For the case of a standing wave, the swash process begins when the shoreline begins to rise from its minimum antinodal position (see Carrier and Greenspan, 1958). In the case of monochromatic waves, the seaward boundary of the swash zone will be fixed and can be readily

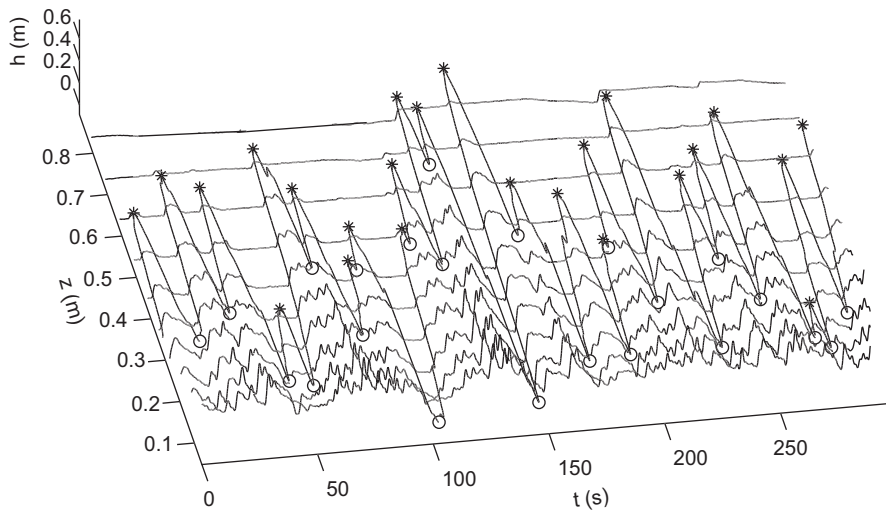


Fig. 3. Time series of runup wire (bold line) and pressure sensor data (thin lines) showing the relationship between shoreline motion and the number of waves reaching various elevations on the beach face. t is time, z is elevation, and h is water depth. Shoreline maxima and minima delimiting individual swash cycles are marked with asterisks and circles, respectively.

identified in either context. On natural beaches, where random breaking short waves (sea and swell) are interacting with non-breaking, standing infragravity waves (leaky-mode and edge waves) a more pragmatic approach is required. Ideally, the range of shoreline excursions associated with both short waves and infragravity waves should be included, but tidal translation should be excluded. The optimal record length to delimit the swash zone is somewhere between 10 and 20 min, depending on the mix of short and long waves driving the swash and the tidal range. In this analysis, record lengths of 15 min have been used on all beaches. Once an appropriate time period is specified, an obvious approach to delimiting the swash zone is to choose the lowest and highest shoreline elevation recorded over that period. The vertical swash extent Z_s is then the difference between these two elevations. To restrict the impact of the occasional extreme event, an alternative approach is to choose the 2.5th and 97.5th percentiles of the shoreline maxima and minima, respectively, which has been the approach used here.

4.2. Delimiting the hydrokinematic regions: outer and inner swash

Using the full 15 min record from which the data shown in Fig. 3 is drawn, Fig. 4 shows several types of tallies presented as either frequency histograms, exceedence frequency curves (EFC) or cumulative

frequency curves (CFC). The tally of times the shoreline moves landward past specified elevations (obtained from the runup wire time series) normalized against the vertical swash extent z/Z_s is presented as a frequency histogram in both Fig. 4a and b (the *uprush histogram*). Very low on the beach there are relatively few times the shoreline moves landward past a specified point, because most swash cycles begin further up the beach. Relatively few instances occur high on the beach either, because most swash cycles do not reach these elevations. The tally of waves that pass specified elevations (obtained from the pressure sensor time series) is presented as an EFC in Fig. 4a (the wave runup height EFC). Note that this is distinct from shoreline run-up height, because not every wave reaches the dry beach to produce shoreline motion. Where the uprush histogram and wave runup height EFC begin to follow each other in trend at point A in Fig. 4a marks the highest elevation where waves overrun pre-existing swash lenses. Below this elevation there are more waves than uprushes of the shoreline, thus not all waves reach the dry beach to produce shoreline motion. Above this elevation, every single wave ultimately produces a single shoreline oscillation. The two curves follow each other but do not converge precisely, because the automated algorithm to pick the number of waves in the pressure records is not perfect. Unfortunately, this imperfection precludes an automated method of identifying point A. It is important to note that point A does

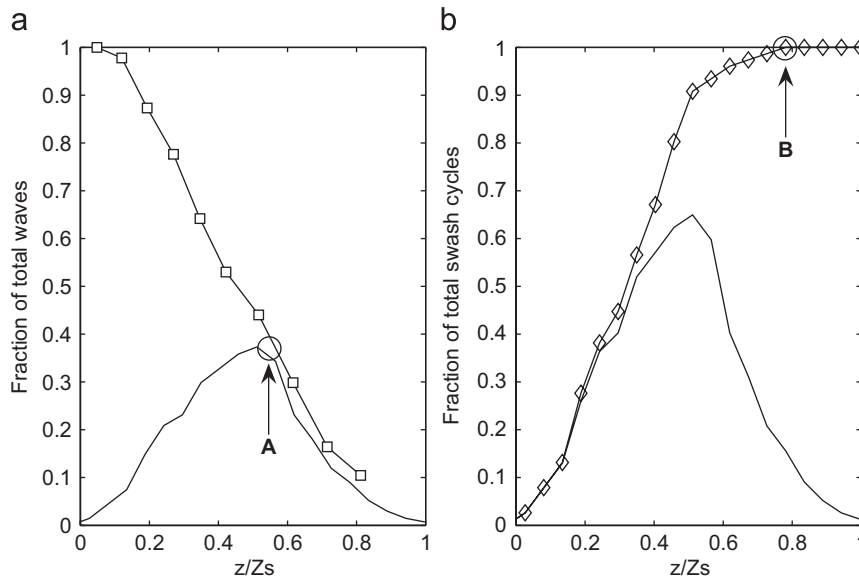


Fig. 4. Demonstration of the method used to delimit the swash zone and locate the boundary between the outer and inner swash. The horizontal axis in both plots is elevation z normalized to the total swash zone extent Z_s ; (a) uprush histogram normalized to total number of waves arriving at the seaward boundary of the swash zone (solid line) plotted together with wave runup height EFC normalized in the same manner (line with squares) and (b) uprush histogram normalized to total number of swash cycles (solid line) plotted together with the shoreline minima CFC normalized in the same manner (line with diamonds).

not mark the landward limit of all wave-swash interactions, only type 1 and 2 interactions.

Fig. 4b shows the uprush histogram together with the tally of shoreline minima occurring below each elevation (obtained from the runup wire time series) presented as a CFC (the shoreline minima CFC). The elevation where the shoreline minima CFC achieves 100% at point B in Fig. 4b (i.e., the elevation of the highest shoreline minima) is the elevation above which there is no type 3 wave-swash interactions. Every shoreline motion landward past this elevation recedes seaward below this elevation without influence from a subsequent wave. Since the landward limit of type 1 and 2 wave-swash interactions always sat further seaward, this elevation point B marks the boundary between the outer and inner swash regions. In the following analysis we sought to reduce the impact of the occasional extreme event, and thus adopted the 97.5th percentile of the shoreline minima CFC rather than the 100th percentile as the boundary between the outer and inner swash.

For wave-swash interactions to occur the phase ratio, ϕ , defined as

$$\phi = \frac{f_{\text{surf}}}{f_{\text{swash}}} \quad (1)$$

must exceed unity. The values of f_{surf} and f_{swash} are the peak frequencies of the inner surf wave spectrum and the shoreline spectrum, respectively. The value of f_{surf} was obtained from the pressure sensor record acquired immediately seaward of the minimum shoreline elevation and in all cases was less than 3 m seaward in the horizontal. The value of f_{swash} was calculated from the runup wire record. For $\phi > 1$ wave-swash interaction should be occurring, whereas for $\phi < 1$ it should be absent. Since natural waves are not monochromatic and ϕ relates only to the peak frequencies of the spectra, many interactions may still occur when $\phi < 1$. However, we might still expect the vertical extent of the outer swash Z_{outer} to scale with the magnitude of ϕ , thus the former is plotted as a function of the latter in Fig. 5a. The former was calculated for each 15 min run collected from a given beach and it is the mean and ± 1 standard deviation for the beach that is plotted. In all cases $\phi > 1$, which is consistent with there being wave-swash interaction and the existence of a outer swash region on all the beaches studied. There is no consistent trend evident in Fig. 5a, however. This simply means that for situations where ϕ is close to unity there will be relatively few wave-swash interactions, but they are spread over a proportion of the

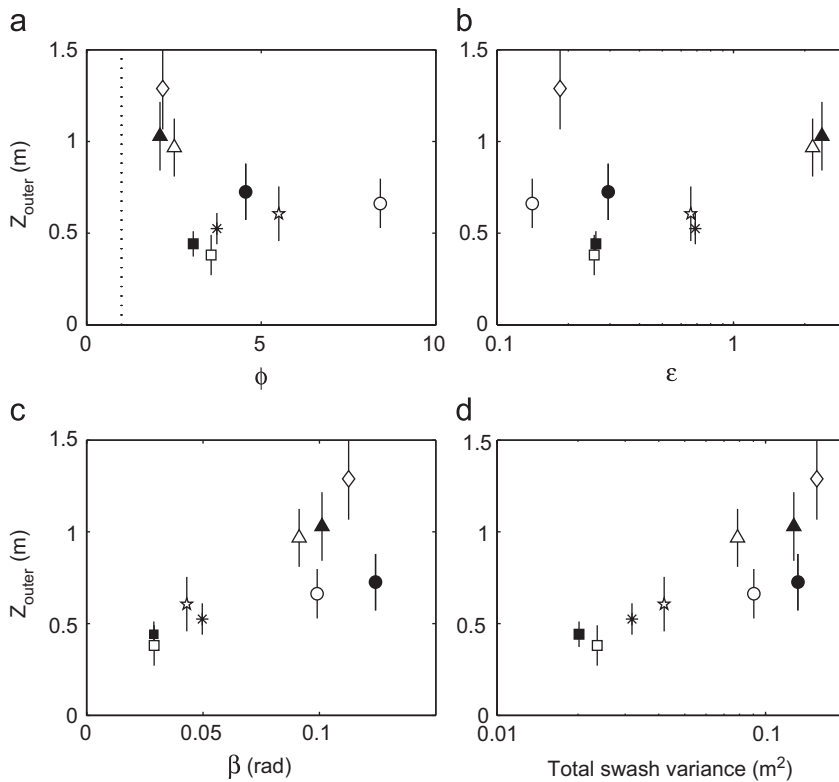


Fig. 5. The mean (± 1 standard deviation) vertical extent of the outer swash Z_{outer} plotted as a function of (a) phase ratio ϕ (Eq. (1)); the vertical dashed line is $\phi = 1$, (b) surf scaling parameter ε (Eq. (2)), (c) beach face slope β , and (d) total swash variance. (Symbols: solid square Seven Mile Beach (July 21), open square Seven Mile Beach (July 22), open star Stradbroke Island, asterisk Moreton Island; open diamond Avoca Beach (October 14), open triangle Avoca Beach (November 16), solid triangle Avoca Beach (November 17), open circle Pearl Beach (cusp embayment), and solid circle Pearl Beach (cusp horn).)

swash zone comparable to situations when ϕ is larger.

Since many other features of surf and swash have been shown to scale with the surf similarity parameter ε , the vertical extent of the outer swash is plotted in Fig. 5b against a ‘spectral version’ of ε given by

$$\varepsilon = \frac{\sqrt{\sigma} \Delta f \omega^2}{g \tan^2 \beta} \quad (2)$$

(after Carrier and Greenspan, 1958). The wave radial frequency $\omega = 2\pi f$ is calculated using the peak frequency of the shoreline elevation spectrum, σ is the corresponding power spectral density at that frequency, Δf is the frequency resolution of the spectrum, g is the gravitational acceleration, and β is the beach face slope angle. The latter was calculated from the planar slope between the maximum runup and rundown limits recorded for each 15 min data run. For monochromatic waves, the shoreline amplitude is used instead of $\sqrt{\sigma} \Delta f$

(e.g., Guza and Bowen, 1976). We chose our approach to avoid making a subjective choice of shoreline amplitude when faced with natural swash containing different mixes of short and long wave energy and with spectral peaks that varied markedly in frequency bandwidth between data runs and between beaches. The values of ε presented here are therefore not quantitatively comparable to most previously published values based on estimates of breaker height or shoreline runup height. The vertical extent of the outer swash is plotted as a function of ε in Fig. 5b, with no trend apparent. The reason for this is evident in Figs. 5c and d where it is plotted as a function of beach slope and shoreline variance, respectively. The latter was calculated by integrating the shoreline spectrum over the range $0.004 < f < 0.5$ Hz. There is a clear positive relationship between the vertical extent of the outer swash and both beach slope and shoreline variance, which is not represented by ε .

The vertical extent of the outer swash normalized against the extent of the total swash zone Z_{outer}/Z_s is plotted as a function of beach slope in Fig. 6. The figure indicates that the former is reasonably independent of beach slope. Based on the full data set, the outer swash on average occupies $53 \pm 21\%$ of the swash zone.

4.3. Methods for identifying relative position in the swash zone

Some previous studies have used the percentage of time that the bed is inundated t_i to indicate the approximate position of instrument stations within the swash zone (Masselink et al., 2005; Aagaard and Hughes, 2006; Masselink and Russell, 2006). The idea being that t_i is expected to decrease with elevation throughout the swash zone. Importantly, it has not yet been established how t_i varies with elevation on natural beaches or how consistent the variation is across different beach types. The relative elevation in the swash zone z/Z_s is plotted as a function of the mean t_i (and ± 1 standard deviation) in Fig. 7. The mean and standard deviations were calculated from the shoreline elevation time series across the entire data set. It is evident from Fig. 7 that the percentage of time that the bed is inundated indeed varies reasonably consistently with elevation in the swash zone across a wide range of beach types. The empirical line of fit

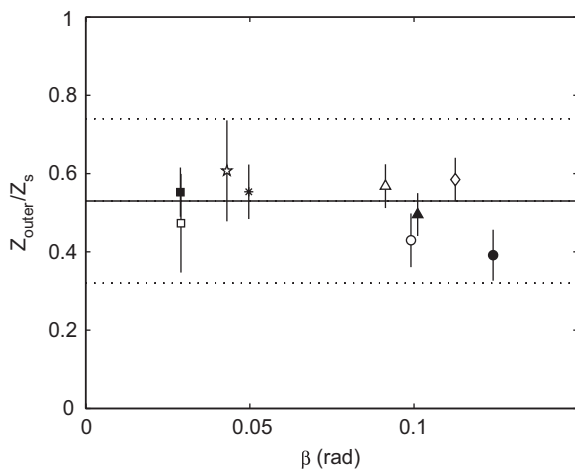


Fig. 6. The mean (± 1 standard deviation) vertical extent of the outer swash Z_{outer} normalized to the total swash zone extent Z_s , plotted as a function of beach slope β . The symbols correspond to different beaches, as listed for Fig. 5. The solid horizontal line is the mean across the entire data set and the dashed line is the corresponding standard error.

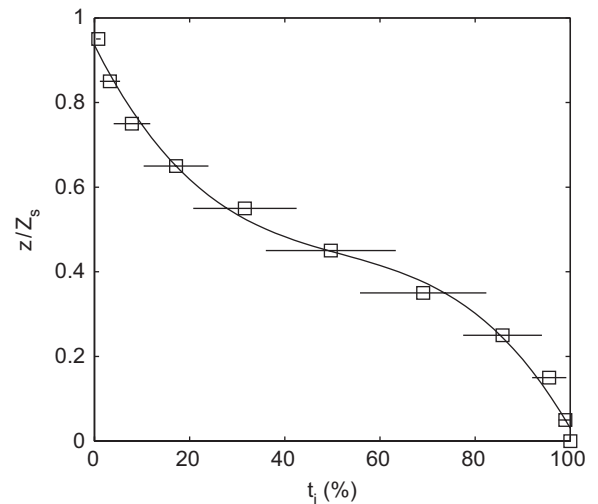


Fig. 7. Relative elevation in the swash zone z/Z_s plotted as a function of the mean (± 1 standard deviation) percentage of time the bed is inundated t_i . The mean and standard deviation were calculated for the entire data set across all beaches. The empirical line of fit is given by Eq. (3).

to the data shown in Fig. 7 is given by

$$\frac{z}{Z_s} = (9.353 \times 10^{-1}) - (2.225 \times 10^{-2})t_i + (3.679 \times 10^{-4})t_i^2 - (2.359 \times 10^{-6})t_i^3. \quad (3)$$

Now that the consistency in variation of t_i across the swash zone has been established, it could be used to locate the position of an instrument station relative to the two hydrokinematic regions. Based on the results shown in Fig. 6, one could solve Eq. (3) for t_i when $z/Z_s = 0.53$. This would provide the probable boundary between the inner and outer swash regions evident in Fig. 6 in terms of the percentage time the bed is inundated. However, this approach suffers from the variance inherent in the data presented here (Fig. 6).

The most direct and accurate approach to determine position relative to the hydrokinematic regions for instrument deployments consisting of a single pressure sensor is to visually inspect the time series of water depth over a stationary time frame (ca. 15 min). If the station is located in the inner swash, the pressure record will consist of isolated swash events separated by periods of zero water depth. The duration of the events will be less than the incident wave period, and during each event there will be only one water depth maximum (viz., the pressure record at P2 in Fig. 1). If the instrument station is in the outer swash, there will

be times when swash events in the pressure record endure longer than the incident wave period and during each swash event there are several water depth maxima (viz., the pressure record at P1 in Fig. 1).

To determine precisely where an instrument station is located within either the inner or outer swash is less straightforward. By using the experimental design described in Section 3.2 plots such as those shown in Figs. 4a and b could be used, but this requires considerable instrumentation that may be peripheral to the experimental goals. We, therefore, provide an approximate approach that requires the deployment of only a single pressure sensor. The bottom panel of Fig. 8 shows the elevation in the outer swash relative to the vertical extent of the outer swash z/Z_{outer} plotted as a function of the ratio of the number of waves W to the number of swash events S . As expected, the ratio W/S decreases towards unity at the top of the outer swash; i.e., $z/Z_{\text{outer}} = 1$. The data obtained from the full range of beaches investigated here indicates that the approximate position of an instrument station in the outer swash region can be determined from the empirical line of fit

$$\frac{z}{Z_{\text{outer}}} = 0.908 - 0.172 \ln(W/S). \quad (4)$$

While there is a considerable amount of natural variability in the data at the seaward end of the outer swash (as $z/Z_{\text{outer}} \rightarrow 0$), there is a sharp decrease in W/S such that the ratio is consistently < 10 for the entire landward half of the outer swash ($z/Z_{\text{outer}} > 0.5$). The top panel of Fig. 8 shows the elevation in the inner swash relative to the vertical extent of the inner swash z/Z_{inner} plotted as a function of the percentage of time the bed is inundated t_i . The approximate position of an instrument in the inner swash region can be determined from the empirical line of fit

$$\begin{aligned} \frac{z}{Z_{\text{upper}}} = & (9.611 \times 10^{-1}) - (1.165 \times 10^{-2})t_i \\ & + (6.433 \times 10^{-3})t_i^2 - (1.344 \times 10^{-4})t_i^3. \end{aligned} \quad (5)$$

5. Discussion

The results presented here are based on the analysis of 147 15 min time series of simultaneously logged resistance wire and pressure sensor data

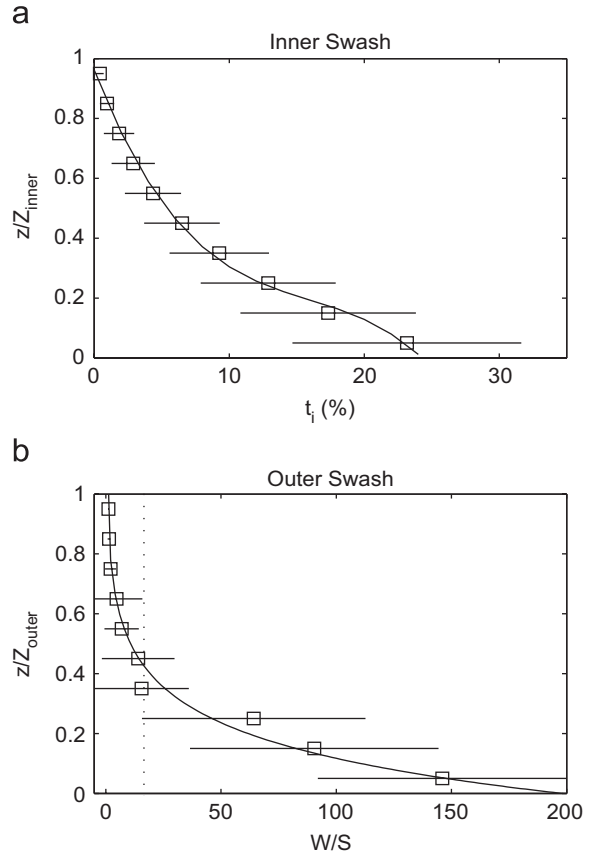


Fig. 8. Demonstration of the method proposed to determine where an instrument station is located within the hydrokinematic regions. The bottom panel shows the elevation in the outer swash region relative to the vertical extent of the outer swash region z/Z_{outer} plotted as a function of the mean (± 1 standard deviation) ratio of number of waves to number of swash events W/S . The vertical dashed line indicates $W/S = 10$. The top panel shows the elevation in the inner swash region z/Z_{inner} plotted as a function of the mean (± 1 standard deviation) percentage of time the bed is inundated t_i . The mean and standard deviations in both cases were calculated for the entire data set across all beaches. The empirical lines of fit are given by Eqs. (4) and (5) for the bottom and top panel, respectively.

obtained from five different swell-dominated, sandy beaches covering the full spectrum of beach states from gently sloping and dissipative to steep and reflective (beach face gradients from 0.03 to 0.12). The range of Iribarren numbers represented in the data here, based on inner surf zone breaker heights, is 0.35–1.4. The results obtained are therefore expected to be generally applicable to most beaches where the swash is driven by a mixture of short (sea and swell) and long waves (leaky mode and edge waves). The results may not apply to beaches where

the swash is driven exclusively by short-period locally generated sea or ultra-dissipative beaches where the swash is driven exclusively by long waves.

5.1. Hydrokinematic nature of the outer and inner swash

At any particular time the bed within the outer swash may be experiencing either inner surf or swash processes, or indeed the two interacting. The outer swash is in fact defined by the presence of wave-swash interactions. In the case of type 1 and 2 interactions, where bores are traveling over an existing swash lens, there will be landward-directed Eulerian flow accelerations with the passage of each overrunning bore. Field measurements have shown that at these times there can also be a landward-directed horizontal pressure gradient and a strong injection of near-bed turbulent kinetic energy (Puleo et al., 2003; Butt et al., 2004; Aagaard and Hughes, 2006). Numerical experiments indicate that the combined effect can significantly enhance sediment mobilization (Calantoni and Puleo, 2006). In the case of type 3 interactions, the significant vertical component of the flow field and turbulence in associated hydraulic jumps can also significantly enhance sediment mobilization (Butt and Russell, 2005). The flow kinematics in this region is clearly complex, and the net sediment flux could be directed either seaward or landward depending on the circumstances (cf. Masselink et al., 2005; Aagaard et al., 2006). The bed everywhere within the inner swash is only subject to pure swash kinematics. Under pure swash driven by breaking waves the velocity skewness is directed offshore, since the uprush duration is shorter than the backwash duration (e.g., Hughes et al., 1997; Hughes and Baldock, 2004; Masselink and Russell, 2006). Moreover, the Eulerian flow accelerations and horizontal pressure gradients are everywhere directed offshore except near the point of bore collapse, which has a typical spatial extent of only 10% or less of the swash length (Hughes and Baldock, 2004; Baldock and Hughes, 2006).

Previous studies that have adopted a swash-by-swash approach to data analysis are based on a dynamic definition of the swash zone extent, i.e., it varies with every wave (e.g., Waddell, 1976; Hughes, 1992; Holland and Puleo, 2001; Puleo and Holland, 2001; Hughes and Baldock, 2004; Baldock and Hughes, 2006). The seaward limit is the point at which the incoming wave arrives at the dry beach

and the landward limit is the maximum vertical shoreline excursion. If an incoming wave is overrunning a preceding swash, the swash motion resulting from that wave does not begin until it overtakes the shoreline and reaches the dry beach ahead. Using this definition, single uninterrupted swash cycles may be selected at any time from instrument stations located in the inner swash, and they can also sometimes be selected from instrument stations located in the outer swash since not all swash cycles are interacting at a given location. Once several single swash cycles are selected, they have typically been ensemble-averaged to obtain statistically robust descriptors of pure swash behavior. It is important to recognize that the spatial extent of such an ensemble-averaged swash does not correspond in any direct way with the swash zone extent defined by a continuous shoreline elevation time series of say 15 min, as described here. A description of swash behavior based on an ensemble average of non-interacting swash cycles will be most representative of flow kinematics in the inner swash, and perhaps also the landward half of the outer swash albeit to a lesser extent. It will be least representative of the flow kinematics at the seaward end of the outer swash, where wave-swash interactions are important most of the time. This may explain, at least in part, why Puleo et al. (2003) argued for the presence of landward-directed flow accelerations in the swash zone and Hughes and Baldock (2004) argued against. The instrument station deployed by the former may have been located in the outer swash, whereas the data presented by the latter is representative of pure swash.

5.2. Significance of the outer swash

The extent of the outer swash has not been investigated to date. The data presented here, from a wide range of beach slopes, indicates that on average it occupies $53 \pm 21\%$ of the swash zone extent. It should be noted that this is based on a rigorous, and thus rather restrictive definition (Fig. 4). The bottom panel of Fig. 8 indicates that for the landward half of the outer swash the number of wave-swash interactions is relatively rare. There is a small hint that the relative extent of the outer swash Z_{outer}/Z_s increases with decreasing beach slope, although, the trend is not significant across the range of this data set (Fig. 6). Observations suggest it is likely that such a trend would be more

evident if highly dissipative beaches were included in the data set. Given that the outer swash is clearly significant in terms of extent, it is appropriate to briefly speculate on its significance from a morphodynamic viewpoint.

To maintain a steady, non-zero beach slope angle the sediment transported by the uprush must balance that transported by the backwash when averaged over a small number of swash cycles. Several mechanisms have been proposed to overcome the offshore-directed velocity skewness and achieve such a balance (see Hughes and Baldock, 2004; Masselink and Puleo, 2006 for recent reviews). Of most interest here is landward sediment advection. During times of increased wave energy, the wave spectrum generally becomes more broad banded leading to increased wave-swash interaction. Kemp (1975) showed that these conditions generally lead to offshore sediment transport. It seems plausible that if the direction of net sediment transport was offshore in the outer swash and hence there was no sediment advection to the inner swash, then velocity skewness in the inner swash would ensure offshore sediment transport occurred across the entire swash zone. The result would be an overall flattening of the beach face profile. If the direction of net sediment transport was onshore in the outer swash, then advection into the inner swash could overcome the offshore-directed velocity skewness, thus resulting in an overall steepening of the beach face profile. Recent models focused on sediment advection in the swash may therefore hold the key to successfully predicting beach face morphodynamics (Pritchard and Hogg, 2005; Alsina et al., 2006). One obstacle at present is that these models do not currently describe wave-swash interactions, and thus cannot predict the direction of net sediment transport in the outer swash.

5.3. Locating instrument stations in the swash zone

The method used here to locate the landward and seaward boundaries of the swash zone was based on shoreline elevation time series obtained from a runup wire. Similar time series can also be obtained from video imagery (e.g., Aagaard and Holm, 1989; Holland et al., 1995). When delimiting the swash zone, we chose to reduce the impact of the occasional extreme event by choosing the landward and seaward boundaries of the swash zone as the 2.5th and 97.5th percentiles of the shoreline minima and maxima CFCs, respectively. This approach is

consistent with morphodynamic observations suggesting implicitly (Holland and Puleo, 2001) and explicitly (Weir et al., 2006) that bed elevation changes in the swash zone tend to be insignificant landward of the elevation exceeded by 2% of runup.

The outer swash is defined here as that region where wave-swash interactions occur and the inner swash is that region where wave-swash interactions are absent. At the boundary between the regions, two conditions must be met: (a) the number of waves arriving at that point equals the number of swash events (i.e., no type 1 and 2 wave-swash interactions occur) and (b) every single shoreline motion landward of that point recedes seaward at least to that point (i.e., no type 3 swash interactions occur). Condition (a) is identified by the coincidence of the uprush histogram and the wave runup height EFC. Condition (b) is identified by the 100th percentile of the shoreline minima CFC. It was found in all cases investigated here that the elevation at which condition (b) was satisfied was always highest, thus a shoreline minima CFC calculated from a shoreline elevation time series is all that is required to locate the boundary between the outer and inner swash.

Fig. 7 shows for the first time the pattern of variation with elevation of the percentage of time that the bed is inundated in the swash zone. The data show that it reduces with elevation in a manner that is consistent across the full range of beaches studied here. Using the percentage of time that an instrument station is inundated, as previous studies have done (e.g., Masselink et al., 2005; Aagaard and Hughes, 2006; Masselink and Russell, 2006), therefore seems to be a valid approach to indicating where the instrument station is located in the swash zone, and Eq. (3) can now be used to quantify the approximate position. However, this approach does not directly indicate which hydrokinematic region the instrument station is located in. While we suggested that it is possible to do so implicitly from the percentage of time the bed is inundated (see Section 4.3), a superior approach, also based only on a single pressure sensor time series, is to determine the ratio of waves to swash events in the time series. It is important to consider the length of time series in this regard. Using a time series that is too short will not incorporate the role of long waves in producing wave-swash interactions, whereas a time series that is too long will incorporate tidal translation of the swash zone. For the swell-dominated, intermediate type, micro-tidal

beaches discussed here that include a range in swash period of ca. 7–120 s, a time series length of 15 min is appropriate. Other conditions may require a different choice. For example, a shorter time series length may be necessary on macrotidal beaches to achieve stationarity with respect to the tide. Similarly, on beaches with long waves of a lower frequency, a longer time series length may be appropriate to include several long wave cycles.

6. Conclusion

Two hydrokinematic regions within the swash zone are identified and delimited. The outer swash region is characterized by wave-swash interactions and the inner swash region is characterized by pure swash motion. The vertical extent of the outer swash region was found to scale directly with inner surf wave variance and beach slope. Since the vertical extent of the entire swash zone also varies directly with inner surf wave variance, the relative extents of the outer and inner swash regions are reasonably constant for a wide range of beach slopes. On average the outer swash occupies approximately 53% of the total swash zone extent, although, wave-swash interactions may be rare at elevations higher than the first 25% of the swash extent. The complex flow kinematics associated with wave-swash interactions will tend to enhance sediment mobility and suspension. The advection of this suspended sediment, either landward or seaward, may play a key role in beach profile behavior.

An approach to delimiting the swash zone and two hydrokinematic regions within this zone, which can be readily applied in field-based research, has been presented. The method determines the swash zone extent over a specified time period that includes all sub-tidal frequencies of shoreline motion, but is stationary with respect to the tide (ca. 15 min). The outer and inner limits of the swash zone can be taken as the lowest minimum and highest maximum in the shoreline elevation time series, respectively. Alternatively, in order to exclude the occasional extreme event, marginal percentiles of the shoreline minima and maxima CFC could be applied (e.g., the 2.5th and 97.5th percentiles). The second approach is consistent with recent morphodynamic studies of the swash zone, which indicate significant bed mobility is generally restricted to this narrower range. The boundary between the outer and inner swash is located at the elevation of the highest minimum in the shoreline

elevation time series. Again, in order to exclude the occasional extreme event, the 97.5th percentile of the shoreline minima cumulative frequency curve could be applied.

To facilitate meaningful comparison of results between future field studies, it is recommended that the pressure record common to most instrument stations deployed in the swash is used to identify which hydrokinematic region the instruments are located in. If the ratio of waves to swash events in a data run $W/S > 10$, then the station is located in the seaward half of the outer swash where wave-swash interactions are dominant. If $1 < W/S < 10$, then it is located in the landward half of the outer swash where wave-swash interactions are present, but not predominant. If $W/S = 1$, then the instrument station is located in the inner swash where wave-swash interactions are absent. Eqs. (4) and (5) could also be used to quantify the approximate elevation within each region, although, the accuracy is far better for the inner swash compared to the outer swash.

Acknowledgments

The Australian Research Council (Grant A10009206) funded many of the experiments reported here. The continued assistance over 10 years in the field from Dave Mitchell (field electronics) is greatly appreciated. Other colleagues who assisted with these experiments at various times include Tom Baldock, Felicia Weir, Peter Nielsen, Nick Cartwright, Matt Tomkins, Tony Peric, Aaron Coutts-Smith, and Diane Horn. The paper has benefited from comments on an earlier draft by Troels Aagaard and two anonymous reviewers for the journal. Thanks also to the anonymous reviewer who suggested the terms outer and inner swash.

References

- Aagaard, T., Holm, J., 1989. Digitization of wave run-up using video records. *Journal of Coastal Research* 5, 547–551.
- Aagaard, T., Hughes, M.G., 2006. Sediment suspension and turbulence in the swash zone of dissipative beaches. *Marine Geology* 228, 117–135.
- Aagaard, T., Hughes, M.G., Møller-Sørensen, R., Andersen, S., 2006. Hydrodynamics and sediment fluxes across an onshore migrating intertidal bar. *Journal of Coastal Research* 22, 247–259.
- Alsina, J.N., Baldock, T.E., Hughes, M.G., Weir, F., Sierra, J.P., 2006. Sediment transport numerical modeling in the swash zone, *Coastal Dynamics 2005*, ASCE.

- Baldock, T.E., Hughes, M.G., 2006. Field observations of instantaneous water slopes and horizontal pressure gradients in the swash zone. *Continental Shelf Research* 26, 574–588.
- Balsillie, J.H., 1985. Redefinition of shore-breaker classification as a numerical continuum and a design shore-breaker. *Journal of Coastal Research* 1, 247–254.
- Butt, T., Russell, P., 2000. Hydrodynamics and cross-shore sediment transport in the swash-zone of natural beaches: a review. *Journal of Coastal Research* 16, 255–268.
- Butt, T., Russell, P., 2005. Observations of hydraulic jumps in high-energy swash. *Journal of Coastal Research* 21, 1219–1227.
- Butt, T., Russell, P., Puleo, J., Miles, J., Masselink, G., 2004. The influence of bore turbulence on sediment transport in the swash and inner surf zones. *Continental Shelf Research* 24, 757–771.
- Calantoni, J., Puleo, J.A., 2006. Role of pressure gradients in sheet flow of coarse sediments under sawtooth waves. *Journal of Geophysical Research* 111, C01010.
- Carrier, G.F., Greenspan, H.P., 1958. Water waves of finite amplitude on a sloping beach. *Journal of Fluid Mechanics* 4, 97–109.
- Elfrink, B., Baldock, T.E., 2002. Hydrodynamics and sediment transport in the swash zone: a review and future perspectives. *Coastal Engineering* 45, 149–167.
- Guza, R.T., Bowen, A.J., 1976. Resonant interactions for waves breaking on a beach. In: *Proceedings 15th International Coastal Engineering Conference*, ASCE, pp. 560–579.
- Guza, R.T., Thornton, E.B., 1981. Wave setup on a natural beach. *Journal of Geophysical Research* 86, 4133–4137.
- Guza, R.T., Thornton, E.B., 1982. Swash oscillations on a natural beach. *Journal of Geophysical Research* 87, 483–491.
- Hegge, B.D., Eliot, I.G., 1991. Swash interactions on sandy beaches. In: *10th Australasian Conference on Coastal and Ocean Engineering*, Water Quality Centre and DSIR Marine and Freshwater, Hamilton, New Zealand, pp. 363–367.
- Holland, K.T., Puleo, J.A., 2001. Variable swash motions associated with foreshore profile change. *Journal of Geophysical Research* 106, 4613–4623.
- Holland, K.T., Raubenheimer, B., Guza, R.T., Holman, R.A., 1995. Runup kinematics on a natural beach. *Journal of Geophysical Research* 100, 4985–4993.
- Hughes, M.G., 1992. Application of a non-linear shallow water theory to swash following bore collapse on a sandy beach. *Journal of Coastal Research* 8, 562–578.
- Hughes, M.G., Turner, I.L., 1999. The beach face. In: Short, A.D. (Ed.), *Handbook of Beach and Shoreface Morphodynamics*. Wiley, pp. 119–144.
- Hughes, M.G., Baldock, T.E., 2004. Eulerian flow velocities in the swash zone: field data and model predictions. *Journal of Geophysical Research* 109, C08009.
- Hughes, M.G., Masselink, G., Brander, R.W., 1997. Flow velocity and sediment transport in the swash-zone of a steep beach. *Marine Geology* 138, 91–103.
- Kemp, P.H., 1975. Wave asymmetry in the nearshore zone and breaker area. In: Hails, J., Carr, A. (Eds.), *Nearshore Sediment Dynamics and Sedimentation*. Wiley-Interscience, pp. 47–67.
- Masselink, G., Puleo, J.A., 2006. Swash zone morphodynamics. *Continental Shelf Research* 26, 661–680.
- Masselink, G., Russell, P., 2006. Flow velocities, sediment transport, and morphological change in the swash zone of a dissipative and reflective beach. *Marine Geology* 227, 227–240.
- Masselink, G., Evans, D., Hughes, M.G., Russell, P., 2005. Suspended sediment transport in the swash zone of a dissipative beach. *Marine Geology* 216, 169–189.
- Nielsen, P., 1989. Wave setup and runup: an integrated approach. *Coastal Engineering* 13, 1–9.
- Puleo, J.A., Holland, K.T., 2001. Estimating swash zone friction coefficients on a sandy beach. *Coastal Engineering* 43, 25–40.
- Puleo, J.A., Holland, K.T., Plant, N.G., Slinn, D.N., Hanes, D.M., 2003. Fluid acceleration effects on suspended sediment transport in the swash zone. *Journal of Geophysical Research* 108, 3350.
- Pritchard, D., Hogg, A.J., 2005. On the transport of suspended sediment by a swash event on a plane beach. *Coastal Engineering* 52, 1–23.
- Shen, M.C., Meyer, R.E., 1963. Climb of a bore on a beach: part 3 run-up. *Journal of Fluid Mechanics* 16, 113–125.
- Synolakis, C.E., 1987. The runup of solitary waves. *Journal of Fluid Mechanics* 185, 523–545.
- Waddell, E., 1976. Swash-groundwater-beach profile interactions. In: Davis, Jr., R.A., Ethington, R.L. (Eds.), *Beach and Nearshore Sedimentation*. Society of Economic Paleontologists and Mineralogists, pp. 115–125.
- Wright, L.D., Short, A.D., 1984. Morphodynamic variability of surf zones and beaches: a synthesis. *Marine Geology* 56, 93–118.
- Weir, F.M., Hughes, M.G., Baldock, T.E., 2006. Beach face and berm morphodynamics fronting a coastal lagoon. *Geomorphology* 82, 331–346.
- Yeh, H.H., Ghazali, A., 1988. On bore collapse. *Journal of Geophysical Research* 96, 6930–6936.